



Published in final edited form as:

*Curr Cancer Drug Targets*. 2019 ; 19(10): 838–851. doi:10.2174/1568009619666190325144636.

## Polyisoprenylated cysteinyl amide inhibitors deplete K-Ras and induce caspase-dependent apoptosis in lung cancer cells

Augustine T. Nkembo<sup>1</sup>, Felix Amissah<sup>1</sup>, Elizabeth Ntantie<sup>1</sup>, Rosemary A. Poku<sup>1</sup>, Olufisayo O. Salako<sup>1</sup>, Offiong Francis Ikpat<sup>2</sup>, Nazarius S. Lamango<sup>1,\*</sup>

<sup>1</sup>College of Pharmacy and Pharmaceutical Sciences, Florida A&M University, Tallahassee, Florida 32307

<sup>2</sup>Department of Pathology, School of Medicine, University of Miami, Miami, FL 33136

### Abstract

**Background:** Non-small cell lung cancers (NSCLC) harboring mutation-induced dysregulation of Ras signaling present some of the most difficult-to-manage cases since directly targeting the constitutively active mutant Ras proteins has not resulted in clinically useful drugs. Therefore, modulating Ras activity for targeted treatment of cancer remains an urgent healthcare need.

**Objective:** In the current study, we investigated a novel class of compounds, the polyisoprenylated cysteinyl amide inhibitors (PCAI), for their anticancer molecular mechanisms using the NSCLC cell panel with K-Ras and/or other mutant genes.

**Method:** The effect of the PCAIs on intracellular K-Ras levels, cell viability, apoptosis, spheroid and colony formation were determined.

**Results:** Treatment of the lung cancer cells with the PCAIs, NSL-RD-035, NSL-BA-036, NSL-BA-040 and NSL-BA-055 resulted in concentration-dependent cell death in both K-Ras mutant (A549, NCI-H460, and NCI-H1573), N-Ras mutant (NCI-H1299) and other (NCI-H661, NCI-H1975, NCI-H1563) NSCLC cells. The PCAIs at 1.0 –10  $\mu$ M induced the degeneration of 3D spheroid cultures, inhibited clonogenic cell growth and induced marked apoptosis via the extrinsic pathway. The most potent of the PCAIs, NSL-BA-055, at 5  $\mu$ M induced a seven-fold increase in the activity of caspase-3/7 and a 75% selective depletion of K-Ras protein levels relative to GAPDH in A549 cells that correlated with PCAIs-induced apoptosis. NSL-BA-040 and NSL-BA-055 also induced the phosphorylation of MAP kinase (ERK 1/2).

**Conclusion:** Taken together, PCAIs may be potentially useful as targeted therapies that suppress NSCLC progression through disruption of Ras-mediated growth signaling.

\* Address correspondences to: Nazarius S. Lamango, Ph.D., College of Pharmacy and Pharmaceutical Sciences, Florida A&M University, Tallahassee, FL 32307, Tel: 850 412-7377 Fax: 850 599-3347, nazarius.lamango@fam.u.edu. Augustine T. Nkembo, Felix Amissah, and Elizabeth Ntantie participated in the design, conduct of the experiments and writing of the manuscript.

Rosemary Poku participated in the analysis of the data.

Olufisayo O. Salako participated in the synthesis of the PCAIs used for the study.

Offiong Francis Ikpat contributed to the research design, interpretation of the results and writing of the manuscript.

Nazarius Lamango conceived the study, supervised the research and writing of the manuscript.

1.5 Conflict of Interest

The authors have no potential conflicts of interest to disclose.

## Keywords

K-Ras; PCAIs; apoptosis; lung cancer

---

## 1.0 Introduction

Members of the Ras superfamily of small GTP-binding proteins mediate signaling pathways that regulate proliferation, differentiation, motility, apoptosis, and metastasis in cancer cells [1,2]. Consequently, their mutations present a challenge to cancer initiation, progression and treatment. For instance, it is known that up to 30% of lung tumors are positive for the K-Ras mutations that render them constitutively active, thereby destroying their ability to function as molecular switches. Their uncontrollable signaling promotes cell survival and proliferation [3,4]. Such mutations have been described in lung adenocarcinomas, a common histological subtype of non-small cell lung cancer (NSCLC) [5,6]. The presence of K-Ras mutations in NSCLC may be associated with shortened survival, time to relapse, disease aggressiveness and/or resistance to drugs [5,7]. Several receptor tyrosine kinases are overexpressed in lung cancer [8–10] resulting in hyperactive growth signaling. These proteins rely on members of the polyisoprenylated GTPases of the Ras family for downstream signaling. Consequently, constitutively active K-Ras mutations by-pass upstream signaling from receptor tyrosine kinase leading to resistance to receptor tyrosine kinase-targeted therapies [11,12].

An effective therapeutic approach towards cancers with KRAS mutations that bypass upstream receptor signaling requires direct targeting of the G-protein. As active K-Ras mutants bind GTP with high affinity, the development of drugs that effectively dislodge the GTP from mutant G-proteins has been a major challenge. Alternative strategies involving targeting other potentially regulatory elements of the proteins have been pursued. These have included attempts targeting the polyisoprenyl modifications that are crucial for the functional localizations and interactions of various members of the oncogenic small GTPases [2,13] through the development of specific inhibitors against the pathway enzymes [14–16]. This has been associated with a limited success [17–19] [20,21].

The lack of effective therapies against cancers driven by mutant Ras proteins coupled with the aggressiveness of such tumors maintains the impetus for the continuous search for novel therapies. This drive led us to develop the polyisoprenylated cysteinyl amide inhibitors (PCAI) initially to suppress the activities of PMPMEase (Aguilar, Nkembo et al. 2014) which we found to be overexpressed in lung and pancreatic cancers [22,23]. Remarkably, we observed that although the PCAIs only minimally inhibited PMPMEase [23], their potencies against cell viability and proliferation, angiogenesis, migration and invasion vastly surpassed their PMPMEase inhibition [24–27]. These findings suggested that the PCAIs were most likely acting through other mechanisms.

Although the hypothesized underlying mechanism for the above-mentioned cellular effects of the PCAIs is the ability of the PCAIs to disrupt the polyisoprenylation-dependent functional interactions, the specific biological processes involved are poorly understood. Functionally, induction of apoptosis by PCAIs is very relevant in cancer therapy since most

of the anticancer agents depend on the elimination of tumor cells by apoptosis. In the current study, we investigated the role of PCAIs in cell cycle arrest, apoptosis and MAP kinase/ERK 1/2 phosphorylation so as to better understand their anti-cancer molecular mechanisms using the NSCLC cell panel harboring mutant K-Ras and/or other mutant growth-regulating genes.

## 1.1 Materials and methods

### 1.1.1 Chemicals and Reagents

PCAI s (NSL-BA-036, NSL-BA-040, NSL-BA-055 and NSL-BA-056) were synthesized in our lab as previously described [23]. CellTiter-Blue Cell Viability Assay kit, Caspase-Glo 3/7, Caspase-Glo 8 and Caspase-Glo 9 Assay kits were obtained from Promega. Paclitaxel, docetaxel, erlotinib, Triton X-100, EDTA, RNase A and antibodies specific to caspase-8, caspase-9, K-Ras were purchased from Sigma Aldrich (St Louis, MO). Annexin V/propidium iodide kits were purchased from EMD Millipore (Temecula, CA). Antibodies specific to caspase-3/7 (Cat. # 9662S), anti-beta-actin monoclonal antibodies (Cat. # 8457S), Alexa Fluor 488-anti-mouse (Cat. # 4408S) and anti-rabbit IgG (Cat. # 4412S) antibodies, and phospho-p44/42 MAPK (ERK1/2) (Thr202/Tyr204) rabbit monoclonal antibody (Cat. # 4370S) were purchased from Cell Signaling (Danvers, MA). Antibodies specific to GAPDH (Cat. # GTX100118) was purchased from GeneTex (Irvine, CA). Horseradish peroxidase-labeled rabbit anti-mouse antibodies (Cat. # sc-358917) were purchased from Santa Cruz Biotechnology (Dallas, TX). Monoclonal anti-K-Ras (Cat. # WH0003845M1), anti-Caspase-8 (Cat. # SAB3500404), anti-Caspase-9 (Cat. # SAB4300693) were obtained from Sigma-Aldrich (St. Louis, MO).

### 1.1.2 Cell culture

The lung cell lines (WI-38, A549, NCI-H1573, NCI-H661, NCI-H460, NCI-H1975, NCI-H1563, and NCI-H1299) and human lung fibroblasts (WI-38) cells were purchased from American Type Culture Collection (Manassas, VA). WI38 cells were cultured in Minimum Essential Medium (Invitrogen, Carlsbad, CA), A549 cells were cultured in F12 Kaighn's Medium (Invitrogen, Carlsbad, CA) and NCI-H1573, NCI-H661, NCI-H460, NCI-H1975, NCI-H1563, and NCI-H1299 cells were cultured in RPMI 1640 (Invitrogen, Carlsbad, CA). All media were supplemented with 10% heat-inactivated fetal bovine serum (Invitrogen, Carlsbad, CA), 100 U/ml penicillin and 100 µg/mL streptomycin (Invitrogen, Carlsbad, CA). The cultures were incubated at 37°C in 5% CO<sub>2</sub>/95% humidified air. In all cases, treatment was done in basal medium supplemented with 5% heat-inactivated fetal bovine serum.

### 1.1.3 Cell viability assay

Cells were seeded at a density of  $2 \times 10^4$  per well in 96-well tissue culture plates and allowed to attach overnight at 37°C in 5% CO<sub>2</sub>/95% humidified air. The cells were then treated with PCAIs (NSL-BA-036, NSL-BA-040, NSL-BA-055, and NSL-BA-056) or paclitaxel, docetaxel, erlotinib and unprenylated cysteinyl amides (NSL-100 and NSL-101). The compounds were dissolved in acetone (solvent, final concentration of 1% in wells). Control cells were treated with 1% acetone of experimental media. Identical amounts of the compounds were used to treat the cells at 24 h for the 48-h exposure. CellTiter-Blue Cell Viability Assay kit (Promega, Madison, WI) was used to determine the cell viability. Cell

viability was expressed as the percentage of the fluorescence in the treated cells relative to that of the controls.

In order to determine the effects of caspase inhibitors on cell viability, A549 lung cancer cells were seeded in 96-well tissue culture plates at a density of  $1 \times 10^4$  per well and allowed to attach overnight at  $37^\circ\text{C}$  in 5%  $\text{CO}_2/95\%$  humidified air incubator. The cells were treated with  $50 \mu\text{M}$  of each of the caspase inhibitors, dissolved in DMSO and returned into the incubator. Two hours later, the cells were further treated with varying concentrations of PCAIs ( $0.2 - 25 \mu\text{M}$ ) dissolved in acetone (final concentration of 1%). Control cells were treated with 1% acetone of experimental medium. Treatment was repeated after 24 hours and cell viability was determined after 48 h using the resazurin reduction assay. Using GraphPad Prism software (San Diego, CA, USA),  $\text{EC}_{50}$  values were determined from non-linear regression plots for cells treated only with caspase inhibitors, PCAIs or both.

#### 1.1.4 Effect of PCAIs on clonogenic cell survival

Cells were seeded into 6-well culture plates at a density of  $5.0 \times 10^4$  cells/well and left at  $37^\circ\text{C}$  for 24 h to attach. The cells were exposed to PCAIs ( $1.0 - 5.0 \mu\text{M}$ ) for 48 h after which the cells were washed with HBSS, trypsinized and counted. The pre-treated cells were then plated at different densities, incubated in fresh drug-free medium containing 10% (v/v) fetal bovine serum for an additional 10 – 14 days. The resulting colonies were fixed with a 10:1 (v/v) mixture of methanol and acetic acid. These were stained with 1% crystal violet and the number of colonies containing 50 or more cells were counted. Cell survival following PCAIs exposure was expressed as the percentage of control survival.

#### 1.1.5 Effect of PCAIs on 3D Cancer Spheroid Cultures

A549 cells were cultured in similar three-dimensional conditions *in vitro* (in which they normally form compact, viable spheroids) and used to determine the effect of the PCAIs. The lung cancer A549 and NCI-H661 cells were seeded at a density of  $2 \times 10^4$  per well in 96-well ultralow-attachment, Lipidure-coat U-shaped clear-bottom plates and allowed to grow overnight at  $37^\circ\text{C}$  in 5%  $\text{CO}_2/95\%$  humidified air. The formed spheroids were then treated with vehicle (1% acetone) or PCAIs ( $1 - 50 \mu\text{M}$ ). Identical amounts of PCAIs were used to supplement the samples at 24 h for the 48 h exposure. The effects of the drugs were captured using the Nikon Eclipse Ti 100 inverted microscope using S Plan Fluor ELWD  $20\times$  Ph1 ADM (numerical aperture = 0.45) with Nikon DS Qi2 camera. CellTiter-Blue Cell Viability Assay kit (Promega, Madison, WI) was used to determine the viability of the spheroids. Cell viability was expressed as the percentage of the fluorescence in the treated cells relative to that of the controls.

#### 1.1.6 Analysis of PCAIs – induced apoptosis

The morphologic analysis, Annexin V/propidium iodide staining was used as per the manufacturer's instructions to study the mode of cancer cell death upon exposure to PCAIs. Cells were seeded into 6-well culture plates at  $2.0 \times 10^5$  cells/well and left at  $37^\circ\text{C}$  for 24 h to attach. Cells were exposed to PCAIs ( $1 - 10 \mu\text{M}$ ) for 48 h followed by washing in PBS and labeling with FITC-conjugated Annexin V for 20 min in the dark. Cells were then

washed and analyzed using a Becton Dickinson FACSsort flow cytometer with CellQuest software (Mansfield, MA).

### 1.1.7 Caspase Assays

A549 cells treated with PCAIs (1 – 5  $\mu\text{M}$ ) for 48 h were used to determine caspase activities and levels of caspase expression. Caspase activities in the cells were determined using Caspase-Glo 3/7, Caspase-Glo and Caspase-Glo 9 Assay kits (Promega, Madison, WI) according to the manufacturer protocol. Briefly, 100  $\mu\text{l}$  caspase-Glo reagent was added and incubated at room temperature for 30 min. The presence of active caspases from apoptotic cells cleaved the aminoluciferin-labeled synthetic tetrapeptide, releasing the substrate for the luciferase enzyme. The caspase activities were measured using a Bio-Tek Gen 5 plate reader (Bio-Tek Instruments, Winooski, VT) caspase activity was expressed as relative luminescence units (RLU)

### 1.1.8 Western Blot Analysis

H1573 and A549 cells ( $2 \times 10^5$  cells/well) grown in tissue culture dish, 60.8  $\text{cm}^2$  (Olympus plastic) purchased from Genesee Scientific (Petersburg, KY) were treated with PCAIs (0 – 5  $\mu\text{M}$ ) for 48 h. Cellular proteins were extracted using Thermo Scientific RIPA lysis and extraction Buffer (25mM Tris-HCl pH 7.6, 150mM NaCl, 1% NP-40, 1% sodium deoxycholate, 0.1% SDS) and halt protease inhibitor cocktail kit mixture. Protein concentration was measured using a Pierce BCA protein quantification assay kit, according to the manufacturer's protocol (Thermo Scientific, Waltham, MA). Lysates containing equal amounts of proteins (40–50  $\mu\text{g}$  of protein) were separated by electrophoresis on a 12% SDS-polyacrylamide gel and then proteins transferred onto polyvinylidene difluoride (PVDF) membranes (0.2  $\mu\text{m}$  pore size, Bio-Rad, Hercules, CA). Membranes were blocked for 1 h at room temperature with blocking buffer (5 % nonfat milk in TBS-T (50 mmol/L Tris-HCl, 150 mmol/L NaCl, and 0.1% Tween 20). All antibodies were diluted with the blocking buffer. The membranes were incubated with K-Ras, caspase-8, caspase-9, caspase-3/7 primary antibody overnight at 4°C. Membranes were then washed and incubated in a solution of TBST containing GAPDH at room temperature for 2 h. After this incubation, the membranes were again washed and the corresponding horseradish peroxidase-conjugated secondary antibody (Santa Cruz Biotechnologies) was added and incubated for 3h at room temperature. Proteins were visualized using the ECL reagent (Bio-Rad, Hercules, CA). Images were captured and protein levels were quantified by densitometry of bands normalized to GAPDH using the Image Lab 6.0 (BioRad, Hercules CA),

### 1.1.9 Immunofluorescence microscopy

A549, H1573 and H661 cells were cultured on 6-well  $\mu$ -slide VI (Ibidi, Fitchburg, WI) at a density of  $3 \times 10^5$  cells/mL at 37°C and 5%  $\text{CO}_2$ /95% humidity and treated with NSL-BA-055 for 48 h. Cells were then fixed with 4% paraformaldehyde for 30 min and then permeabilized for 30 min with 0.3% Triton X-100 before being blocked with 1% BSA in PBS for 30 min. After blocking, cells were incubated overnight at 4°C with K-Ras (10  $\mu\text{g}/\text{ml}$ , Sigma Aldrich) or GAPDH (GeneTex) primary antibodies. Secondary antibodies conjugated with Alexa Fluor 488-anti-mouse IgG (Cell Signaling) were incubated for 24 h at 4°C. Before imaging, cells were stained with DAPI. Images were captured at room

temperature on a Nikon Eclipse *Ti* Microscope at 40× magnification. The brightness and contrast were adjusted with Nikon NIS-Elements software for optimal images acquisition. All operations on the control image (untreated cells) were replicated to the images of the treated cells to allow for accurate comparisons of fluorescent intensities and cropping (using the same area). Images were copied as a single image from a stack and pasted as a picture (enhanced metafile) for publication. The FITC intensity for each cell was quantified as the mean sum intensity per cell and plotted using GraphPad Prism.

#### 1.1.10 Effect of PCAs on MAPK activation

A549 cells ( $2 \times 10^6$  in 60.8 cm<sup>2</sup> wells) were seeded overnight and treated with the indicated concentrations of NSL-BA-040 and NSL-BA-055 for 48 h. They were rinsed with PBS, lysed with RIPA buffer mixed with 0.1% v/v cocktail of protease inhibitors. SDS-PAGE sample buffer was immediately added to the samples followed by boiling for 5 min. The samples were then analyzed by western blot for P44/42 MAPK and  $\beta$ -Actin for the effect of PCAs on their phosphorylation levels using the phospho-p44/42 MAPK (ERK1/2) (Thr202/Tyr204) as the primary antibody.

#### 1.1.11 Statistical analysis

All results were expressed as the means  $\pm$  S.E.M. The concentration–response curves were obtained by plotting the percentage inhibition against the log of the inhibitor concentrations. Nonlinear regression plots were generated using GraphPad Prism version 5.0 for Windows (San Diego, CA). From these, the concentrations that inhibits cell viability by 50% (EC<sub>50</sub>) were calculated. Statistical significance was determined by either One-way ANOVA with Dunnett's post-hoc test or by Student's T-test as indicated in figure legends. P-values of less than 0.05 were considered statistically significant.

## 1.2 Results

### 1.2.1 PCAs inhibit lung cancer cell viability and clonogenic cell survival.

PCAs were originally designed to inhibit PMPMEase activity. However, this inhibitory effect occurred at relatively higher concentration compared to most of the biological effects observed based on previous studies on pancreatic cancer cells [23]. We therefore examined the effect of PCAs on the viability of an array of lung cancer cell lines. Treatment of cells with PCAs for 48 h resulted in a significant concentration-dependent decrease in cell viability compared with untreated cells (Fig. 1A). As shown in Table 2, the EC<sub>50</sub> for the PCAs, NSL-BA-040 and NSL-BA-055 were the most potent with EC<sub>50</sub> values ranging from as low as 1.1 to 6.2  $\mu$ M. The most susceptible cell line is the NCI-H1573 cells, adenocarcinoma (stage 4 disease) which harbors K-Ras mutation (EC<sub>50</sub> of 1.8 and 1.1  $\mu$ M for NSL-BA-040 and NSL-BA-055 respectively). In general, PCAs were more effective at inhibiting cell viability relative to Docetaxel, Erlotinib and Paclitaxel (Table 2). To assess the impact of the polyisoprenyl group on the potency of the PCAs, cysteinyl amides lacking the polyisoprenyl moiety (NSL-100 and NSL-101) were used as a negative control on A549 cells. The unprenylated cysteinyl amides (NSL-100 and NSL-101) were less effective at inducing cell death (EC<sub>50</sub> greater than 50 and 45  $\mu$ M respectively, compared to the PCAs (Fig. 1B).

We further examined the cytotoxic effect of PCAIs in colony formation assays. We used these assays to assess the ability of the PCAIs to prevent tumor relapse after treatment. As shown in Figs. 2A and B, NSL-BA-040 and NSL-BA-055 induced concentration dependent inhibition of clonogenic cell survival on the cell lines studied. Fig. 2B shows the survival curves in terms of residual colony number. The number of colonies treated with PCAIs was significantly reduced at concentrations higher than 1  $\mu\text{M}$ . The inhibition of colony numbers was concentration-dependent (Fig. 2A) with significantly limited colony formation on exposure to 5  $\mu\text{M}$  PCAIs in all the cell lines used. These results are consistent with the effects of PCAIs on cell viability.

### 1.2.2 PCAIs prevents spheroid formation

To better observe drug response characteristics in a system that better simulates the *in vivo* situation of tumors, the effect of PCAIs were studied using 3D spheroids culture [28,29]. As shown in Fig. 3, NSL-BA-040 and NSL-BA-055 prevented compact spheroids from being formed as well as induced degeneration of already established spheroids generated with either A549 or H661 cells. The induction of spheroid degeneration and cell death occurred at relatively higher concentrations (9.3  $\mu\text{M}$  and 6.2  $\mu\text{M}$  for NSL-BA-040 and NSL-BA-055, respectively) compared to the 2D monolayer culture of the A549 cells (5.2  $\mu\text{M}$  and 5.6  $\mu\text{M}$  for NSL-BA-040 and NSL-BA-055, respectively) as indicated in Fig. 3A. PCAIs at low micro-molar concentrations (0 – 0.5  $\mu\text{M}$ ) prevented spheroid formation (results not shown).

### 1.2.3 PCAIs induce apoptosis in A549 and H661 cells

We investigated the mode of cell death induced by the PCAIs in A549 and H661 cells by measuring Annexin V-positive cells using flow cytometry analysis (Fig. 4). As shown in Fig. 4A and B, exposure to varying concentrations of PCAIs (0 – 10  $\mu\text{M}$ ) resulted in higher population of early and late apoptotic cells (3.0 $\pm$ 0.3% to 99.3 $\pm$ 0.1% in A549 cells; 3.7 $\pm$ 1.0% to 81.3 $\pm$ 11.3% in H661 cells) compared to untreated control (2.0 $\pm$ 0.1% for A549 and 2.6 $\pm$ 0.4% for H661) for NSL-BA-040. We also observed concentration-dependent increments of late apoptotic population when cells were exposed to the PCAIs. We evaluated the concentration-dependent effects on the late apoptotic population of A549 (1.2 $\pm$ 0.3%, 14.8 $\pm$ 7.8%, 42.2 $\pm$ 6.8%, 91.7 $\pm$ 2.8%) and H661 cells (5.5 $\pm$ 4.2%, 27.0 $\pm$ 6.6%, 53.7 $\pm$ 4.3%, 96.9 $\pm$ 0.3%) when treated with NSL-BA-055 (1.0, 2.0, 5.0 or 10  $\mu\text{M}$ ). Less than 1% (A549) or 10% (H661) of the cell population showed necrotic signs when treated with 10  $\mu\text{M}$  of PCAIs.

### 1.2.4 PCAIs induced-apoptosis involves caspase activation

The complex process of apoptosis mobilizes different proteins via caspase-dependent or caspase-independent pathways. Caspase-dependent pathway may be either the extrinsic or intrinsic pathway which involves the activation of caspase-8 or caspase-9, respectively. Either pathway ultimately terminates with the activation of caspase-3/7 which executes downstream DNA cleavage molecules. We investigated the molecular mechanism underlying the PCAI-induced apoptotic process by employing proluminescent substrates, which produce luminescence upon cleavage by caspase as well as immunoblotting techniques using caspase specific antibodies. In the caspase-glo assays, treated cells were stained cells with aminoluciferin-labeled substrate of caspase and the caspase-3/7, -8, -9 activities were

determined by measuring the luminescence intensities. As shown in Fig. 5A, we observed a concentration related increase in caspase-8 and caspase-3/7 activities in A549 cells treated with 1.0 – 5.0  $\mu\text{M}$  of PCAIs. The increase in activity of caspase-3/7 and 8 was especially more significant in NSL-BA-055 treated cells, suggesting that NSL-BA-055 was more effective at inducing activation of extrinsic caspase pathway in A549 lung cancer cell line. Moreover, NSL-BA-055 suppressed the activity of caspase-9, indicating that the apoptotic effects of the PCAIs are mediated by caspase-8 through the extrinsic pathway. These data were confirmed with western blot analysis which showed an increase in the levels of caspase-8, caspase-3/7 proteins but not caspase-9 following 48 h treatment with PCAIs (Fig. 5B).

When A549 cells were treated with the PCAIs or caspase inhibitors alone or in combination, the caspase inhibitors increased the  $\text{EC}_{50}$  values for NSL-BA-040 by 82% (caspase 1), 18% (caspase 3), 0% (caspase 8) and 490% (caspase 9) over cells treated with NSL-BA-040 alone. For cells treated with NSL-BA-055 and caspase inhibitors, the  $\text{EC}_{50}$  values were elevated only in those cells that were co-treated with caspase 9 inhibitor (92%) over cells treated only with NSL-BA-055. The difference between the two PCAIs co-treated with the caspase inhibitors may be due to the higher potency of NSL-BA-055 over NSL-BA-040. Cells treated with caspase inhibitors alone also decreased cell viability with  $\text{EC}_{50}$  values that were at least 100-fold higher than those for the PCAIs.

### 1.2.5 PCAIs significantly reduce K-Ras protein level expressions in lung cancer

Small GTPases of the Ras and Rho families regulate cell proliferation and migration. Targeting of these proteins in the treatment of cancer has been limited due to the lack of agents that specifically suppress their levels and/or activities without major side effects. We previously showed that PCAIs diminish the levels of the Rho proteins to suppress cell migration and invasion [26]. Since K-Ras is a major regulator of cell proliferation, we investigated the effects of PCAIs on the levels of the K-Ras protein. PCAIs diminished the levels of K-Ras in both Western blotting and immunocytochemical analysis (Fig. 6 and 7). The effects of the PCAIs on the levels of the K-Ras protein in Western blotting assays was most significant in A549 cell lines where 2  $\mu\text{M}$  NSL-BA-040 elicited a 50% decrease and 5  $\mu\text{M}$  NSL-BA-055 induced a 75% decrease in the levels of the K-Ras protein compared to controls (Fig. 6A). In the H1573 cell line, we observed a trend towards decrease in the levels of K-Ras with PCAIs exposure, however, this decrease was not statistically significant compared to control (Fig. 6B). In agreement with the Western blotting results, we observed a concentration-dependent decrease in the fluorescent intensities of K-Ras in H1573, H661 and A549 cells that were exposed to NSL-BA-055 (Fig. 7). Whereas NSL-BA-055 did not significantly alter the fluorescent intensity of GAPDH, a cytosolic housekeeping protein, it markedly diminished the fluorescent intensity of the K-Ras protein. Exposure to 2  $\mu\text{M}$  NSL-BA-055 resulted in an 80%, 60% and 85% decrease in normalized K-Ras (K-Ras/GAPDH) fluorescent intensity in A549 (Fig. 7A), H1573 (Fig. 7B), and H661 (Fig. 7C) cells, respectively. Taken together, these data demonstrate that PCAIs exposure suppresses the levels of K-Ras in a panel of non-small cell lung cancer cells.



### 1.2.6 PCAIs stimulate MAPK phosphorylation

When A549 cells were treated with the PCAIs and probed for MAPK (ERK1/2) phosphorylation, it was observed that phosphorylated MAPK that was barely observable in the untreated controls increased immensely in a concentration-dependent manner following treatment with 1 to 5  $\mu\text{M}$  of NSL-BA-040 (Fig. 8). This increase was only when the cells were treated with 1  $\mu\text{M}$  of NSL-BA-055. This is more likely due to the more potent nature of NSL-BA-055 which likely caused a more rapid degradation of proteins in the cell than the less potent NSL-BA-040. This is corroborated by the loss of  $\beta$ -actin when the cells were treated with 2 and 5  $\mu\text{M}$  concentrations of NSL-BA-055 (Fig. 8).

### 1.3. Discussion

Tumor development and metastasis comprises a complex process that include sustaining of proliferative signaling, evasion of growth suppression, evasion of apoptosis, enabling of replicative immortality, induction of angiogenesis and activation of invasion and metastasis [30,31]. These processes are often termed the “hallmark of cancer.” Cancer cells dysregulate their signaling to ensure the growth and survival potentials. A lot of effort has been geared towards the development of therapeutic agents that shut off a hallmark capability, however these efforts have yielded limited success due to drug resistance. In some instances, tumor cells were found to develop resistance to a previously potent angiogenic inhibitor by shifting their dependence on the angiogenesis hallmark capability to heightened invasion and metastasis; another hallmark capability [32–34]. It is thus very likely that effective strategies in the treatment of cancers may require therapeutic agents that simultaneously attenuate the signaling pathways that regulate growth/proliferation, apoptosis, angiogenesis, invasion and metastasis. Moreover, a balance between proliferative versus death signals is tightly regulated in normal cells and dysregulated in cancer cells. Agents that tip this balance to foster cell death and suppress cell growth/proliferation may be more successful in the treatment of cancers.

We recently demonstrated that a novel class of compounds, the PCAIs, block angiogenesis in both *in vitro* and *in vivo* models of angiogenesis [24] and disrupted the F-actin cytoskeleton to suppress lung cancer cell migration and invasion [26]. In this study, we investigated the effects of PCAIs on lung cancer cell viability and survival and report that the PCAIs (1) suppress the viability of a panel of lung cancer cell line monolayers and spheroids, (2) induce G1 cell cycle arrest and cell death by apoptosis, (3) suppress the levels of oncogenic K-Ras protein, and (4) suppress survival of lung cancer cells in both 2D and 3D cultures.

To further assess the anti-survival effects of PCAIs, we examined the viability of a panel of lung cancer cells grown as monolayers or spheroids. In these assays, we observed a dose-dependent inhibition of the viability of several NSCLC cell lines irrespective of their p53 or K-Ras status. The p53 protein is a tumor suppressor that regulates uncontrolled growth, whereas K-Ras is an oncogene that fosters cell growth. The PCAIs suppressed the viability of cells harboring both wildtype and mutant forms of both proteins. Control compounds lacking the farnesyl moiety present in PCAIs did not elicit similar effects at inhibiting cell viability indicating that the farnesyl moiety in PCAIs is important and essential for the

PCAI-mediated effects on cell viability. To gauge the clinical potential of the PCAs, we compared their potency to the chemo-agents; docetaxel, paclitaxel, and to the EGFR inhibitor, Erlotinib, all three agents being anti-cancers drugs currently in clinical use for the treatment of lung cancer. PCAs induced cell death at concentrations ( $EC_{50}$ ) that were at least  $50 \times$  lower than the concentration of docetaxel,  $10 \times$  lower than the concentration of paclitaxel, and  $200 \times$  lower than the concentration of erlotinib required to elicit similar effects. Chemo-agents include DNA-interacting drugs that inhibit DNA replication and destroy cells at different phases of the cell cycle. These agents are non-specific and thus toxic to both normal and cancerous cells. Erlotinib, an inhibitor of EGFR signaling acts upstream of K-Ras, thus cancers harboring constitutively active K-Ras mutants are resistant to erlotinib. The ability of the PCAs to inhibit the viability of lung cancer cells is not surprising as the PCAs were designed to mimic the polyisoprenylated form of this protein. The farnesyl moiety in the PCAs may thus disrupt interactions of the K-Ras protein with its binding partners thereby suppressing the viability of cancer cells. Cell death induced by PCAs may thus be target specific and such a mode of cell death may limit the side-effects present with the use of chemo-agents. The PCAs' effects on the WI-38 cells was comparable to the effects on the lung cancer cells. This was expected as normal cells also require polyisoprenylated proteins for their normal cellular functions. This does not however mean that the PCAs cannot be used as anticancer agents as they have been shown to be cytostatic and antiangiogenic at submicromolar concentrations [24]. The ability of the PCAs to block angiogenesis while being cytostatic is potentially beneficial for anticancer therapy as angiogenesis is required for nutrient supply to feed the growing tumor and only a few other physiological processes in adults such as wound healing. These features make them more selective against tumor growth. Furthermore, novel strategies for selectively targeting agents to various cancer cell types that overexpress cell surface receptors for internalization is an area of active research that is rendering indiscriminately cytotoxic agents more selective towards cancer cells [35].

The aforementioned observation that the PCAs inhibit the viability of NSCLC cells, led us to investigate the mechanism by which the PCAs cause the death of these cells. Programmed cell death or apoptosis is orchestrated by a series of committed signaling events that ultimately lead to the activation of proteases known as caspases [36]. There are two major mechanisms by which cells undergo apoptosis; the death receptor (extrinsic) and mitochondrial (intrinsic) pathways. One major difference between these pathways lies in the initiator caspase. The death receptor mechanism is initiated by caspase-8 whereas the mitochondrial mechanism is initiated by caspase-9. Both pathways eventually lead to the activation of executioner caspase-3/7. Investigations into the PCAs-induced mechanism of cell death revealed that exposure to the PCAs resulted in the activation of caspase-8 while co-incubation of the PCAs with caspase inhibitors revealed the greatest reversal of apoptosis with the caspase-9 inhibitor. These results show that both pathways may be involved in the PCAs-induced apoptosis.

In addition to inducing apoptosis, inhibiting proliferation, suppressing survival, angiogenesis and invasion, an effective cancer agent must have chemo-preventive properties to avoid tumor relapse. We investigated the chemo-preventive effects of PCAs in assays where we pre-treated NSCLC cells with PCAs and then examined their survival and growth to form

colonies or spheroids in the absence of PCAIs. In these assays, the PCAIs markedly suppressed cell survival, growth and formation of colonies and spheroids indicating that the PCAIs have the potential to be effective chemo-preventive agents. We also previously demonstrated that the PCAIs diminished the levels of the Rho GTPases, RhoA, Cdc42 and Rac1 to suppress cell migration and invasion [26] and blocked angiogenesis in both *in vitro* and *in vivo* models of angiogenesis [24]. Ras signaling is well-known to regulate proliferation, survival, and angiogenesis [7,37–39]. We thus investigated if the PCAIs diminish the levels of K-Ras to suppress proliferation, survival and angiogenesis. As predicted, we observed a significant decrease in the levels of the K-Ras protein upon exposure to PCAIs. This decrease in the levels of K-Ras that disrupts major signaling pathways such as the Raf/MEK/ERK and PI3K that regulate cell proliferation, survival, and angiogenesis thus making the PCAIs efficient anti-proliferative, anti-survival and anti-angiogenic agents.

Cancers harboring K-Ras mutations are some of the deadliest cancers. Mutations in the K-Ras gene are present in 25–35% of all newly diagnosed non-small cell lung cancers, with a higher proportion in the adenocarcinoma subtype [40,41]. Mutations in K-Ras abrogates the GTPase activity of the protein, resulting in a hyperactive K-Ras protein that constitutively turns on signaling pathways pertaining to growth, proliferation, survival and suppression of apoptosis [3,4]. Targeting hyperactive K-Ras as a strategy in the treatment of cancer has been investigated with limited success [42]. In most of these studies, these inhibitors block the K-Ras metabolic pathway and its regulatory proteins [43–45]. Agents that attenuate K-Ras signaling while directly altering the levels of the protein may constitute an effective therapeutic strategy in the treatment of lung cancer as K-Ras ablation using gene therapy in mice and cancer cells have demonstrated profound anti-tumorigenic phenotypes [46,47]. The mechanism by which the levels of K-Ras are suppressed is presently unclear. It could be that the PCAIs fork out K-Ras from its polyisoprenyl-cysteine-mediated interactions with other proteins thereby exposing it to degradation. Studies with polyisoprenylated small molecules have previously been shown to speed up polyisoprenylated protein degradation [48,49]. Given that the PCAIs also promote ERK 1/2 phosphorylation, which are proteins whose effects on gene expression are central to their functional mechanism and whose activities are preceded upstream by Ras proteins, the observed depletion of K-Ras may also be due to gene suppression as a feedback inhibition mechanism.

ERK 1/2 activation is typically associated with increased cell proliferation, migration and invasion [50]. It was therefore interesting to observe that the PCAIs, rather than suppressing their phosphorylation, instead promoted it. These findings are however consistent with numerous other studies showing that various agents induced apoptosis through phosphorylation-mediated activation of ERK 1/2 [51–53]. The responses to various RAF-MEK-ERK signaling have been reported to vary depending on which isoforms of the three proteins are complexed together on the scaffold proteins as well as the localization of the complexes. Scaffold proteins with activated MEK-ERK complexes bound to the Golgi apparatus interact only with cytosolic substrates while transcriptional effects of ERK 1/2 require translocation into the nucleus where they phosphorylate transcriptional factors [51].

In summary, we demonstrate that PCAIs, by diminishing the levels and thus activity of the K-Ras protein, disrupt its downstream pathways (Raf/MEK/ERK and PI3K), thereby suppressing cell growth, proliferation, survival and angiogenesis while promoting the activation of death receptor signaling pathways to induce caspase-dependent apoptosis. As previously mentioned, the six major hallmarks of cancer are self-sufficiency in growth signals, insensitivity to anti-growth signals, evasion of apoptosis, limitless replicative potential, induction of angiogenesis and activation of invasion and metastasis. Our previous work [24,25] and current work indicate that the PCAIs inhibit growth, induce apoptosis, suppress angiogenesis, invasion and metastasis. Collectively, these results indicate that the PCAIs attenuate at least four of the six major hallmark capabilities and underscore their potential usefulness as effective agents in anti-cancer strategies.

## Acknowledgement

The research reported in this publication was supported by the National Cancer Institute (NCI) and National Institute of General Medical Sciences (NIGMS) of the National Institutes of Health (NIH) under Grant SC1CA190505 and by the National Institute on Minority Health and Health Disparities (NIMHD) of the NIH under Award Number G12 MD007582 (previous award NIH/NCRR/RCMI G12 RR03020). The content is solely the responsibility of the authors and does not necessarily represent the official views of the National Institutes of Health.

## List of Abbreviations

<b>NSCLC</b>	non-small-cell lung cancer
<b>PMPMEase</b>	polyisoprenylated methylated protein methyl esterase
<b>PPMTase</b>	polyisoprenylated protein methyl transferase or isoprenyl carboxylmethyl transferase (icmt)
<b>PCAIs</b>	polyisoprenylated cysteinyl amide inhibitors

## References

1. Flotho C, Kratz C, Niemeier CM: Targeting ras signaling pathways in juvenile myelomonocytic leukemia. *Curr Drug Targets* (2007) 8(6):715–725. [PubMed: 17584027]
2. Schubert S, Shannon K, Bollag G: Hyperactive ras in developmental disorders and cancer. *Nat Rev Cancer* (2007) 7(4):295–308. [PubMed: 17384584]
3. Mills NE, Fishman CL, Scholes J, Anderson SE, Rom WN, Jacobson DR: Detection of k-ras oncogene mutations in bronchoalveolar lavage fluid for lung cancer diagnosis. *Journal of the National Cancer Institute* (1995) 87(14):1056–1060. [PubMed: 7616596]
4. Ridanpaa M, Karjalainen A, Anttila S, Vainio H, Husgafvelpursiainen K: Genetic alterations in p53 and k-ras in lung-cancer in relation to histopathology of the tumor and smoking history of the patient. *International journal of oncology* (1994) 5(5):1109–1117. [PubMed: 21559688]
5. Westcott PM, To MD: The genetics and biology of kras in lung cancer. *Chinese journal of cancer* (2013) 32(2):63–70. [PubMed: 22776234]
6. Ding L, Getz G, Wheeler DA, Mardis ER, McLellan MD, Cibulskis K, Sougnez C, Greulich H, Muzny DM, Morgan MB, Fulton L et al.: Somatic mutations affect key pathways in lung adenocarcinoma. *Nature* (2008) 455(7216):1069–1075. [PubMed: 18948947]
7. Mascaux C, Iannino N, Martin B, Paesmans M, Berghmans T, Dusart M, Haller A, Lothaire P, Meert AP, Noel S, Lafitte JJ et al.: The role of ras oncogene in survival of patients with lung cancer: A

- systematic review of the literature with meta-analysis. *British journal of cancer* (2005) 92(1):131–139. [PubMed: 15597105]
8. Ballas MS, Chachoua A: Rationale for targeting vegf, fgf, and pdgf for the treatment of nsclc. *OncoTargets and therapy* (2011) 4(43–58. [PubMed: 21691577]
  9. Kasahara K, Arao T, Sakai K, Matsumoto K, Sakai A, Kimura H, Sone T, Horiike A, Nishio M, Ohira T, Ikeda N et al.: Impact of serum hepatocyte growth factor on treatment response to epidermal growth factor receptor tyrosine kinase inhibitors in patients with non-small cell lung adenocarcinoma. *Clin Cancer Res* (2010) 16(18):4616–4624. [PubMed: 20679350]
  10. Huang L, Fu L: Mechanisms of resistance to egfr tyrosine kinase inhibitors. *Acta pharmaceutica Sinica* (2015) 5(5):390–401. [PubMed: 26579470]
  11. Molina JR, Adjei AA: The ras/raf/mapk pathway. *Journal of thoracic oncology : official publication of the International Association for the Study of Lung Cancer* (2006) 1(1):7–9.
  12. John T, Liu G, Tsao MS: Overview of molecular testing in non-small-cell lung cancer: Mutational analysis, gene copy number, protein expression and other biomarkers of egfr for the prediction of response to tyrosine kinase inhibitors. *Oncogene* (2009) 28 Suppl 1(S14–23. [PubMed: 19680292]
  13. Sebti SM: Protein farnesylation: Implications for normal physiology, malignant transformation, and cancer therapy. *Cancer Cell* (2005) 7(4):297–300. [PubMed: 15837619]
  14. Ghobrial IM, Adjei AA: Inhibitors of the ras oncogene as therapeutic targets. *Hematol Oncol Clin North Am* (2002) 16(5):1065–1088. [PubMed: 12512383]
  15. Winter-Vann AM, Casey PJ: Post-prenylation-processing enzymes as new targets in oncogenesis. *Nat Rev Cancer* (2005) 5(5):405–412. [PubMed: 15864282]
  16. Ohkanda J, Knowles DB, Blaskovich MA, Sebti SM, Hamilton AD: Inhibitors of protein farnesyltransferase as novel anticancer agents. *Curr Top Med Chem* (2002) 2(3):303–323. [PubMed: 11944822]
  17. Cox AD, Der CJ, Philips MR: Targeting ras membrane association: Back to the future for anti-ras drug discovery? *Clin Cancer Res* (2015) 21(8):1819–1827. [PubMed: 25878363]
  18. Gibbs JB, Oliff A, Kohi NE: Farnesyltransferase inhibitors: Ras research yields a potential cancer therapeutic. *Cell* (1994) 77(175–178. [PubMed: 8168127]
  19. Agrawal AG, Somani RR: Farnesyltransferase inhibitor as anticancer agent. *Mini Rev Med Chem* (2009) 9(6):638–652. [PubMed: 19519490]
  20. Ma YT, Gilbert BA, Rando RR: Inhibitors of the isoprenylated protein endoprotease. *Biochemistry* (1993) 32(9):2386–2393. [PubMed: 8443178]
  21. Court H, Amoyel M, Hackman M, Lee KE, Xu R, Miller G, Bar-Sagi D, Bach EA, Bergo MO, Philips MR: Isoprenylcysteine carboxylmethyltransferase deficiency exacerbates kras-driven pancreatic neoplasia via notch suppression. *The Journal of clinical investigation* (2013) 123(11):4681–4694. [PubMed: 24216479]
  22. Amissah F, Duverna R, Aguilar BJ, Poku RA, Kiros GE, Lamango NS: Polyisoprenylated methylated protein methyl esterase overexpression and hyperactivity promotes lung cancer progression. *Am J Cancer Res* (2014) 4(2):116–134. [PubMed: 24660102]
  23. Aguilar BJ, Nkembo AT, Duverna R, Poku RA, Amissah F, Ablordeppey SY, Lamango NS: Polyisoprenylated methylated protein methyl esterase: A putative biomarker and therapeutic target for pancreatic cancer. *Eur J Med Chem* (2014) 81(323–333. [PubMed: 24852279]
  24. Nkembo AT, Ntantie E, Salako OO, Amissah F, Poku RA, Latinwo LM, Lamango NS: The antiangiogenic effects of polyisoprenylated cysteinyl amide inhibitors in huvec, chick embryo and zebrafish is dependent on the polyisoprenyl moiety. *Oncotarget* (2016) 7(42):68194–68205. [PubMed: 27626690]
  25. Nkembo AT, Salako O, Poku RA, Amissah F, Ntantie E, Flores-Rozas H, Lamango NS: Disruption of actin filaments and suppression of pancreatic cancer cell viability and migration following treatment with polyisoprenylated cysteinyl amides. *Am J Cancer Res* (2016) 6(11):2532–2546. [PubMed: 27904769]
  26. Ntantie E, Fletcher J, Amissah F, Salako OO, Nkembo AT, Poku RA, Ikpat FO, Lamango NS: Polyisoprenylated cysteinyl amide inhibitors disrupt actin cytoskeleton organization, induce cell rounding and block migration of non-small cell lung cancer. *Oncotarget* (2017) 8(19):31726–31744. [PubMed: 28423648]

27. Poku RA, Salako OO, Amissah F, Nkembo AT, Ntantie E, Lamango NS: Polyisoprenylated cysteinyl amide inhibitors induce caspase 3/7- and 8-mediated apoptosis and inhibit migration and invasion of metastatic prostate cancer cells. *Am J Cancer Res* (2017) 7(7):1515–1527. [PubMed: 28744401]
28. Friedrich J, Seidel C, Ebner R, Kunz-Schughart LA: Spheroid-based drug screen: Considerations and practical approach. *Nature protocols* (2009) 4(3):309–324. [PubMed: 19214182]
29. Friedrich J, Ebner R, Kunz-Schughart LA: Experimental anti-tumor therapy in 3-d: Spheroids--old hat or new challenge? *International journal of radiation biology* (2007) 83(11–12):849–871. [PubMed: 18058370]
30. Hanahan D, Weinberg RA: The hallmarks of cancer. *Cell* (2000) 100(1):57–70. [PubMed: 10647931]
31. Hanahan D, Weinberg RA: Hallmarks of cancer: The next generation. *Cell* (2011) 144(5):646–674. [PubMed: 21376230]
32. Azam F, Mehta S, Harris AL: Mechanisms of resistance to antiangiogenesis therapy. *European Journal of Cancer* (2010) 46(8):1323–1332. [PubMed: 20236818]
33. Ebos JML, Lee CR, Kerbel RS: Tumor and host-mediated pathways of resistance and disease progression in response to antiangiogenic therapy. *Clinical Cancer Research* (2009) 15(16):5020–5025. [PubMed: 19671869]
34. Bergers G, Hanahan D: Modes of resistance to anti-angiogenic therapy. *Nature Reviews Cancer* (2008) 8(8):592–603. [PubMed: 18650835]
35. Wang CW, Wang Y, Tortorella M, Ojima I: Design, synthesis and preclinical study of novel taxoid-based small molecule drug conjugates (smdcs) using folate/dimethyltetrahydrofolate (dmthf) as tumor targeting module. *Abstr Pap Am Chem S* (2017) 253(
36. Pistritto G, Trisciuglio D, Ceci C, Garufi A, D’Orazi G: Apoptosis as anticancer mechanism: Function and dysfunction of its modulators and targeted therapeutic strategies. *Aging-U.S* (2016) 8(4):603–619.
37. Molina JR, Adjei AA: The ras/raf/mapk pathway. *Journal of Thoracic Oncology* (2006) 1(1):7–9. [PubMed: 17409820]
38. Shapiro P: Ras-map kinase signaling pathways and control of cell proliferation: Relevance to cancer therapy. *Crit Rev Cl Lab Sci* (2002) 39(4–5):285–330.
39. Kranenburg O, Gebbink MFBG, Voest EE: Stimulation of angiogenesis by ras proteins. *Bba-Rev Cancer* (2004) 1654(1):23–37.
40. Kris MG, Johnson BE, Kwiatkowski DJ, Iafrate AJ, Wistuba II, Aronson SL, Engelman JA, Shyr Y, Khuri FR, Rudin CM, Garon EB et al.: Identification of driver mutations in tumor specimens from 1,000 patients with lung adenocarcinoma: The nci’s lung cancer mutation consortium (lcmc). *Journal of Clinical Oncology* (2011) 29(18).
41. Barlesi F, Blons H, Beau-Faller M, Rouquette I, Ouafik L, Mosser J, Merlio JP, Bringuier PP, Jonveaux P, Le Marechal C, Denis MG et al.: Biomarkers (bm) france: Results of routine egfr, her2, kras, braf, pi3kca mutations detection and eml4-alk gene fusion assessment on the first 10,000 non-small cell lung cancer (nslc) patients (pts). *Journal of Clinical Oncology* (2013) 31(15).
42. Berndt N, Hamilton AD, Sebt SM: Targeting protein prenylation for cancer therapy. *Nature reviews Cancer* (2011) 11(11):775–791.
43. Rao S, Cunningham D, de Gramont A, Scheithauer W, Smakal M, Humblet Y, Kourteva G, Iveson T, Andre T, Dostalova J, Illes A et al.: Phase iii double-blind placebo-controlled study of farnesyl transferase inhibitor r115777 in patients with refractory advanced colorectal cancer. *Journal of Clinical Oncology* (2004) 22(19):3950–3957. [PubMed: 15459217]
44. Van Cutsem E, de Velde HV, Karasek P, Oettle H, Vervenne WL, Szawlowski A, Schoffski P, Post S, Verslype C, Neumann H, Safran H et al.: Phase iii trial of gemcitabine plus tipifarnib compared with gemcitabine plus placebo in advanced pancreatic cancer. *Journal of Clinical Oncology* (2004) 22(8):1430–1438. [PubMed: 15084616]
45. Blumenschein G, Ludwig C, Thomas G, Tan E, Fanucchi M, Santoro A, Crawford J, Breton J, O’Brien M, Khuri F: A randomized phase iii trial comparing ionafarnib/carboplatin/paclitaxel

versus carboplatin/paclitaxel (cp) in chemotherapy-naive patients with advanced or metastatic non-small cell lung cancer (nslc). *Lung Cancer* (2005) 49(S30–S30).

46. Singh A, Greninger P, Rhodes D, Koopman L, Violette S, Bardeesy N, Settleman J: A gene expression signature associated with “k-ras addiction” reveals regulators of emt and tumor cell survival. *Cancer cell* (2009) 15(6):489–500. [PubMed: 19477428]
47. Fisher GH, Wellen SL, Klimstra D, Lenczowski JM, Tichelaar JW, Lizak MJ, Whitsett JA, Koretsky A, Varmus HE: Induction and apoptotic regression of lung adenocarcinomas by regulation of a k-ras transgene in the presence and absence of tumor suppressor genes. *Genes & development* (2001) 15(24):3249–3262. [PubMed: 11751631]
48. Kloog Y, Gana-Weisz M, Niv H, Elad G, Marciano D, Haklai R: Dislodgment and accelerated degradation of ras. *Neurosci Lett* (1997) S28–S28.
49. Haklai R, Weisz MG, Elad G, Paz A, Marciano D, Egozi Y, Ben-Baruch G, Kloog Y: Dislodgment and accelerated degradation of ras. *Biochemistry-Us* (1998) 37(5):1306–1314.
50. Busca R, Pouyssegur J, Lenormand P: Erk1 and erk2 map kinases: Specific roles or functional redundancy? *Front Cell Dev Biol* (2016) 4(
51. Mebratu Y, Tesfaigzi Y: How erk1/2 activation controls cell proliferation and cell death is subcellular localization the answer? *Cell Cycle* (2009) 8(8):1168–1175. [PubMed: 19282669]
52. Lu ZM, Xu SC: Erk1/2 map kinases in cell survival and apoptosis. *Iubmb Life* (2006) 58(11):621–631. [PubMed: 17085381]
53. Kim HS, Lim GY, Hwang J, Ryoo ZY, Huh TL, Lee S: Induction of apoptosis by obovatol as a novel therapeutic strategy for acute myeloid leukemia. *Int J Mol Med* (2014) 34(6):1675–1680. [PubMed: 25319672]

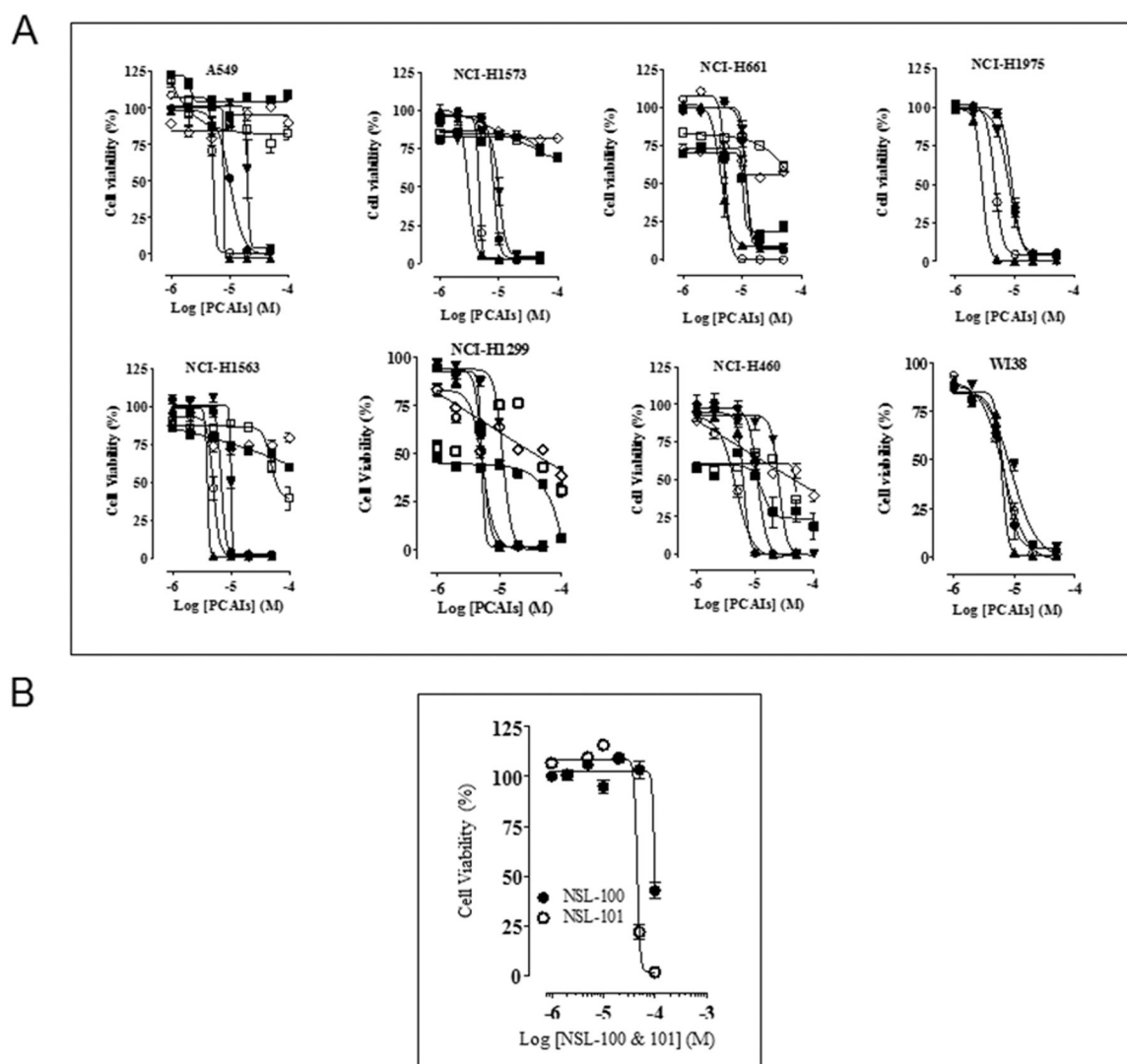


**Figure 1. PCAIs inhibit lung cancer cell viability.**

(A) Human lung cancer (A549, NCI-H1573, NCI-H661, NCI-H460, NCI-H1975, NCI-H1563, and NCI-H1299) and human lung fibroblasts (WI-38) cells were cultured and seeded in 96-well plates at a density of  $2 \times 10^4$  per well and allowed to attach overnight at  $37^\circ\text{C}$  in 5%  $\text{CO}_2/95\%$  humidified air. Cells were then treated with either 1 – 50  $\mu\text{M}$  of PCAIs (● NSL-BA-036, ○ NSL-BA-040, ▲ NSL-BA-055, ▼ NSL-BA-056) or (■) Paclitaxel, (□) Docetaxel and ( ) Erlotinib for 48 h as described in the methods. Cell viability was determined after the final treatment by fluorescence using the resazurin reduction assay. Each point represents the mean  $\pm$  SEM relative to the control untreated cells. (B) To evaluate the importance of the polyisoprenyl moiety on cytotoxicity, A549 cells were assayed as described in (A) above, except cells were treated with NSL-100 and NSL-101. These compounds have a similar structure to the PCAIs but lack the polyisoprenyl moiety.



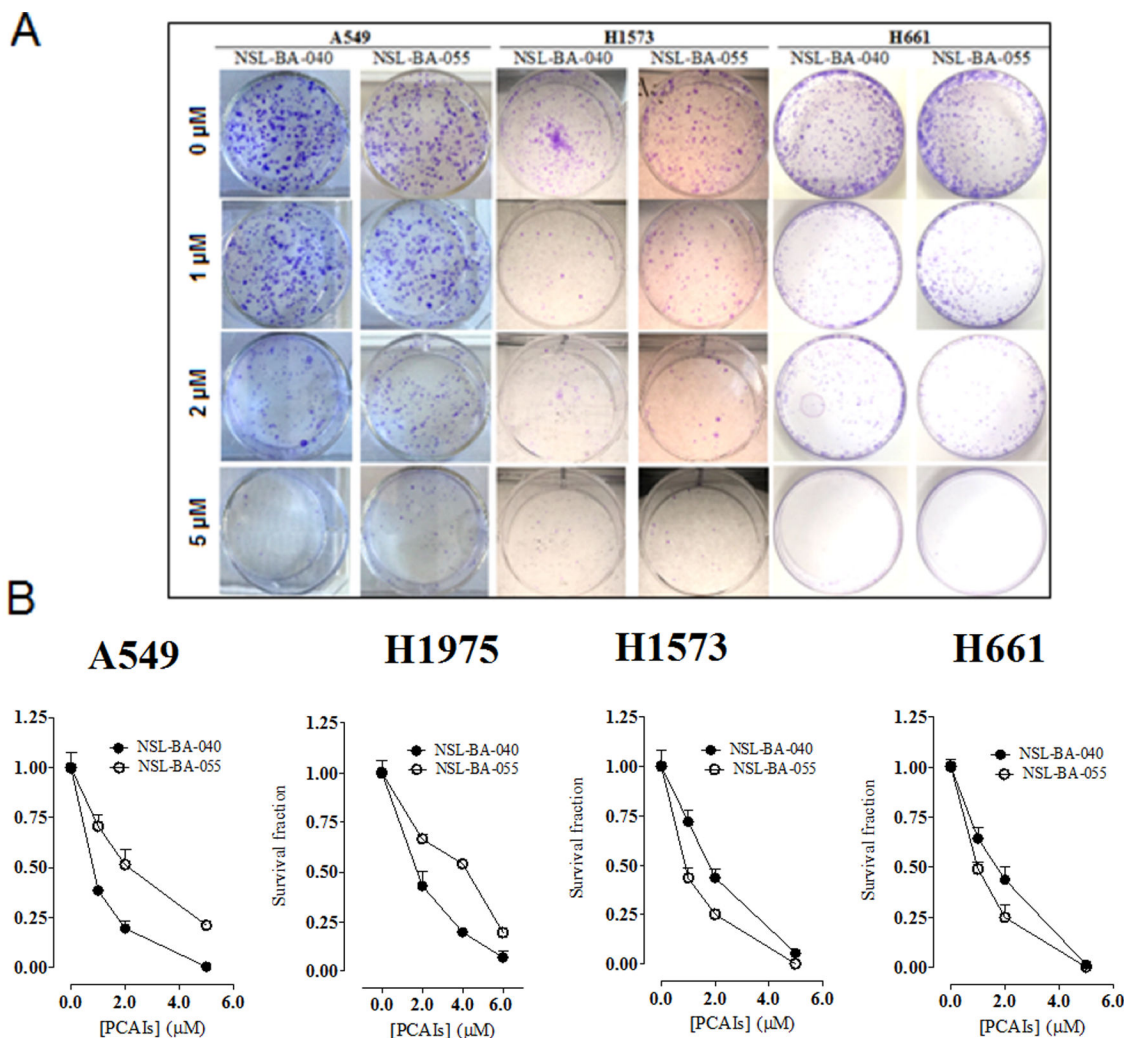
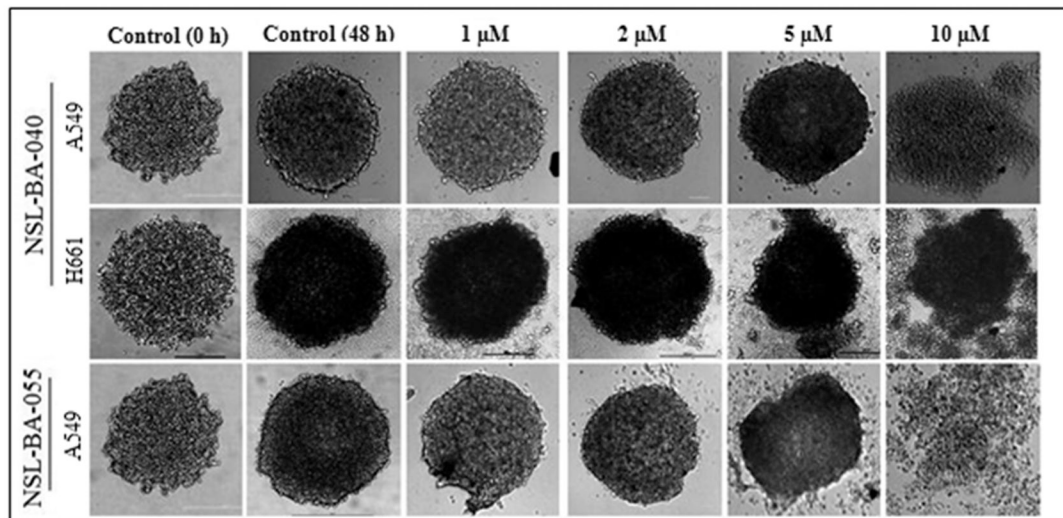


**Figure 2. Clonogenic cell death caused by PCAIs.**

Lung cancer cells in culture were treated with PCAIs (1 – 5 μM) for 48 h, washed, trypsinized, counted and cultured in the absence of PCAIs for a further 12–14 days at 37°C. Cells that survived formed colonies which were fixed and stained with crystal violet. Representative images of colonies were captured (A) and then clonogenic survival was determined (B). The results are expressed as the means (± SEM, N = 4) relative to the controls. Significance (\*\*\*)  $p < 0.001$  was determined by Student’s t-test.

A



B

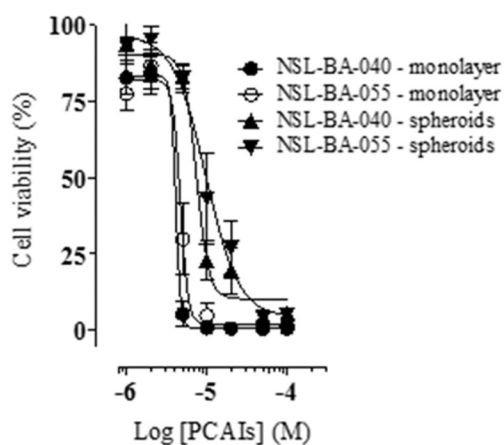


**Figure 3. PCAIs induce degeneration of 3D spheroid cultures.**

A549 and H661 cells plated at 20,000 cells/well in a low-attachment, U-shaped, black clear-bottom plates. Images were acquired 24 h post-plating and 48 h after treatment. Representative images of spheroids treated with different PCAIs concentrations are shown in (A). Spheroids treated with high concentrations of PCAIs appear to disintegrate. Cell viability was determined after the final treatment with PCAIs (1 – 50  $\mu\text{M}$ ) by fluorescence using the resazurin reduction assay in (B). The  $\text{EC}_{50}$ s were higher in the spheroids (7.4 and 9.7  $\mu\text{M}$  for NSL-BA-040 and NSL-BA-055, respectively) compared to that of the 2D culture for both compounds (4.1 and 4.7  $\mu\text{M}$  for NSL-BA-040 and NSL-BA-055, respectively). Each point represents the mean  $\pm$  SEM relative to the control untreated cells.

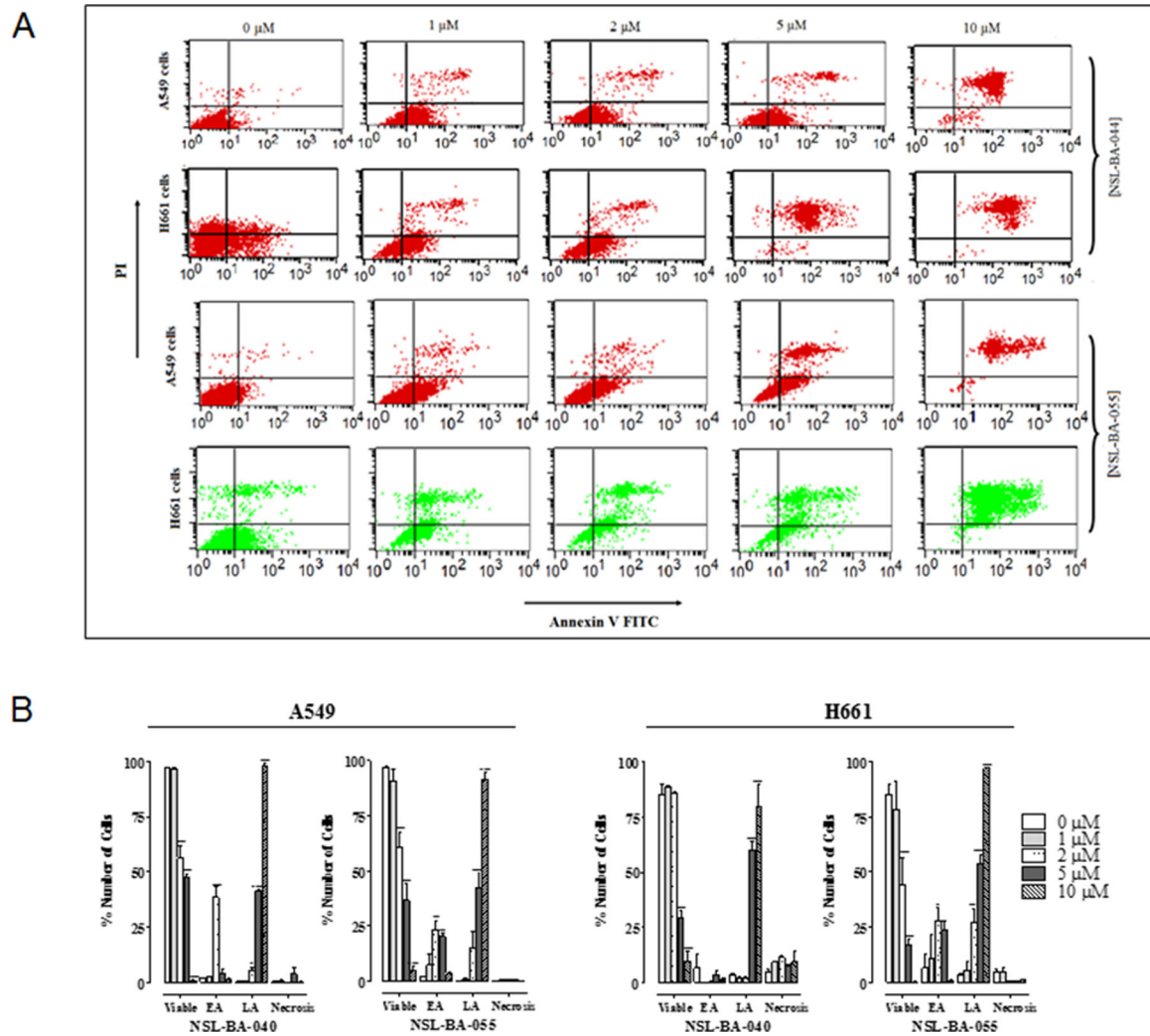


**Figure 4. PCAIs induce apoptosis.**

A549 and H661 cells treated with PCAIs (1 – 10  $\mu\text{M}$ ) for 48 h were examined for externalization of phosphatidylserine using Annexin V-FITC and flow cytometry. PCAI treatment promoted an increase in the number of cells with an increased Annexin V-FITC fluorescence prior to the loss of membrane integrity in early apoptosis (lower right-hand quadrant) and late apoptosis (upper right-hand quadrant). The dot plots (A) represent a single experiment while the graph (B) is an average from 3 independent experiments.

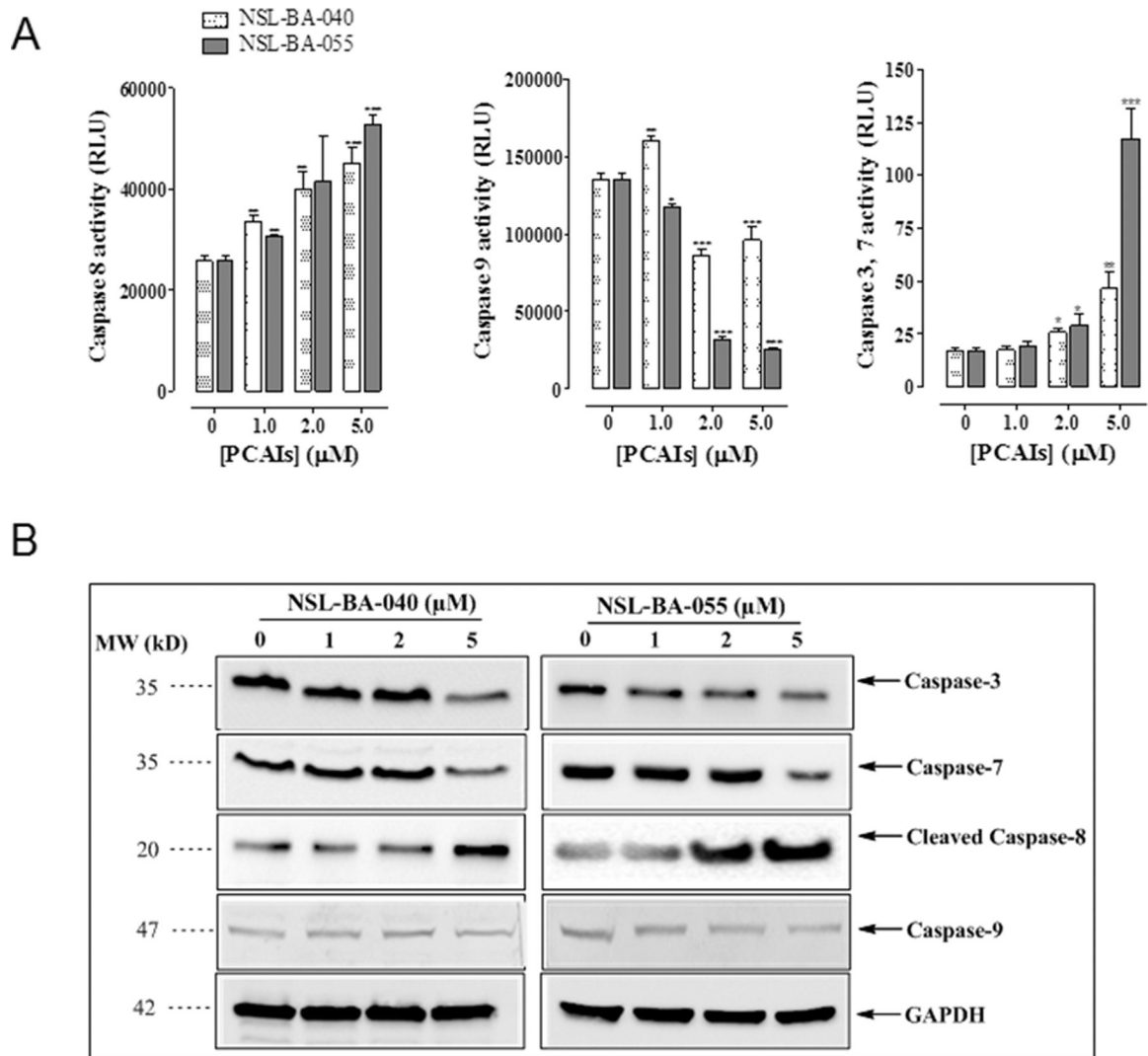


**Figure 5. PCAIs-induced apoptosis is mediated by Caspase-8 and Caspase-3/7.**

(A) A549 cells were seeded at 5000/well for Caspase-3/7 assay and 30,000/well for both Caspase-8 and 9 assays in a white-walled 96-well plate for 24 h before start of experiment. PCAIs (1–5  $\mu\text{M}$ ) or 1  $\mu\text{L}$  of acetone (carrier solution) were then added to triplicate wells. Identical amounts of PCAIs were used to supplement the samples at 24 h for 48 h exposure. Caspase activity was determined after 48 h incubation with Caspase-glo luminescent assay according to manufacturer's instructions. Data on relative luminescence units (RLU) are expressed as mean  $\pm$  S.D. Significance (\* $p < 0.05$ , \*\* $p < 0.01$ , \*\*\* $p < 0.001$ ) was determined by Student's t-test. (B) A549 cells ( $2 \times 10^5$  cells/well) grown in 100 mm tissue culture dishes were treated with PCAIs (0–5  $\mu\text{M}$ ) for 48 h. Cell lysates were generated using RIPA lysis buffer, protein concentration was determined and lysates containing equal amounts of proteins were separated by gel electrophoresis and proteins transferred onto polyvinylidene difluoride (PVDF) membranes. Membrane-bound proteins were probed with antibodies against caspase-8, caspase-9, caspase-3/7, GAPDH and visualized using HRP-conjugated secondary antibodies and ECL reagents.

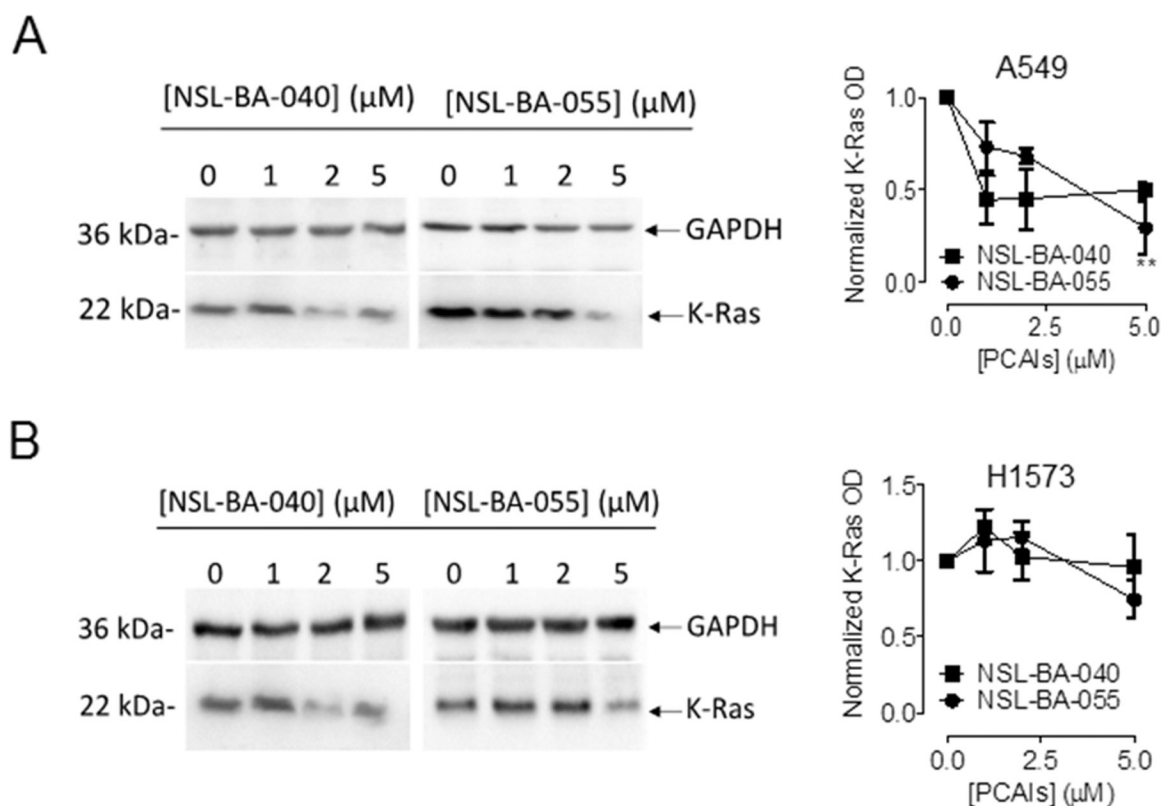


**Figure 6. PCAIs diminish K-Ras protein levels in lung cancer cells.**

Whole cell lysates of lung cancer cells, A549 and H1573 treated for 24 h with PCAIs (0–5  $\mu\text{M}$ ) were analyzed by western blot for K-Ras protein levels expression as described in the Materials and Methods. Briefly, 40–50  $\mu\text{g}$  of whole cell lysate proteins were loaded into the wells of 12% gels and subjected to SDS-PAGE electrophoresis. Proteins were then transferred unto PVDF membranes and membranes were immunoblotted for K-Ras and GAPDH. Densitometry of bands was performed using Image Lab Software and normalized to GAPDH. Data are representative of three independent experiments. Statistical significance (\*\* $p < 0.01$ ) was determined by 1-way ANOVA with post hoc Dunnett's test.

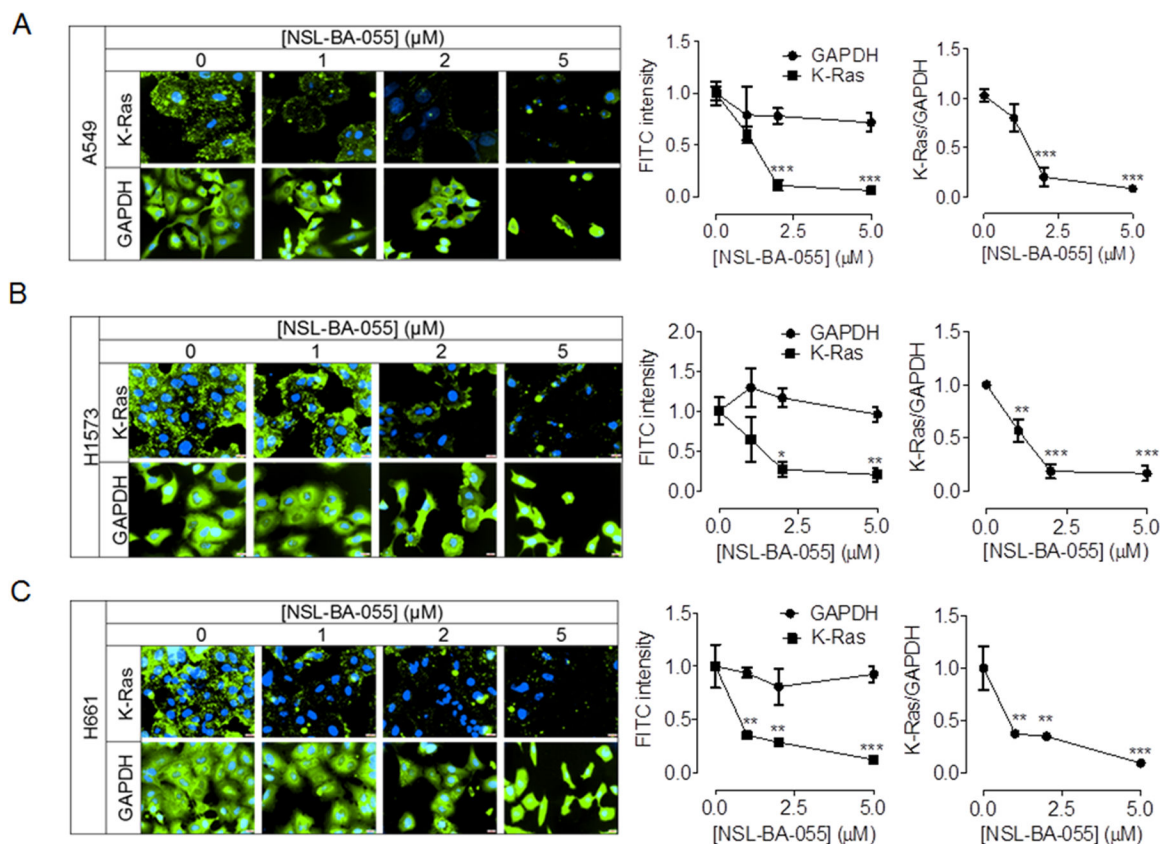


**Figure 7. NSL-BA-055 promotes loss of K-Ras in lung cancer cells.**

Adherent cells (H1573, H661 and A549 cell lines) were treated, fixed using 4% formaldehyde, and probed for K-Ras, GAPDH as described in Materials and Methods. Images were captured on a Nikon Eclipse Ti Microscope at 40× magnification. Nikon NIS-Elements software was used to quantify the mean fluorescent intensities per cell. Fluorescent intensity shown in graphs are mean ± SEM of N = 50 –100 cells and are representative of three independent experiments. Statistical comparison between untreated controls and treated groups were determined by 1-way ANOVA with Dunnett’s post-test comparisons. Significance was defined as \*P < 0.05; \*\*P < 0.01 and \*\*\*P < 0.001.

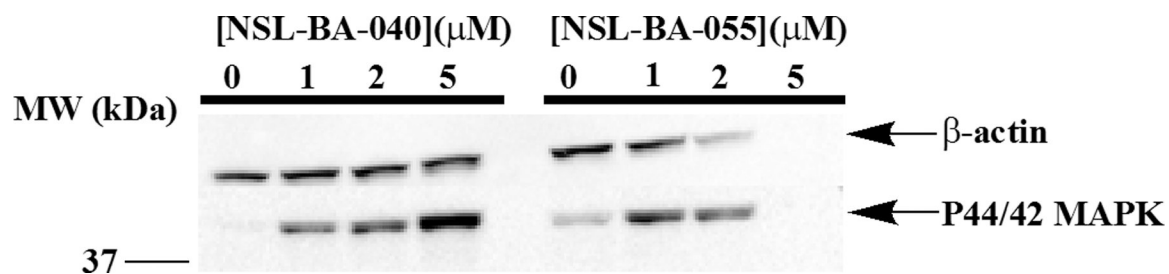


**Figure 8. PCAIs stimulate MAPK phosphorylation in A549 cells.**

Cells ( $2 \times 10^6$  in  $60.8 \text{ cm}^2$  wells) were seeded overnight and treated with the indicated concentrations of NSL-BA-040 and NSL-BA-055 for 48 h. They were rinsed with PBS, lysed with RIPA buffer mixed with 0.1% v/v cocktail protease inhibitors and SDS-PAGE sample buffer immediately added and boiled. The samples were then analyzed by western blot for P44/42 MAPK and  $\beta$ -Actin levels. Note the depletion of proteins in the samples treated with the more potent NSL-BA-055 likely due to apoptosis.

**Table 1:**

NSCLC cell lines used in this study.

ATCC® No.	Name	Histology	Tumor Source	Mutant Gene
CCL75™	WI38	Normal	Lung	
CCL-185™	A549	Carcinoma	explant culture of lung carcinomatous tissue	KRAS - G12S (c.34G > A)
CRL-5803™	NCI-H1299	Large cell carcinoma	metastasis, lymph node	NRAS - Q61K (c.181C > A)
CRL-5875™	NCI-H1563	Non-small-cell lung carcinoma (NSCLC)	primary	CDKN2A
HTB-177™	NCI-H460		lung: pleural effusion	KRAS - Q61H (c.183A > T)
HTB-183™	NCI-H661	Large cell carcinoma	metastasis, lymph node	CDKN2A SMARCA4 TP53
CRL-5877™	NCI-H1573	Adenocarcinoma	metastasis, soft tissue	KRAS
CRL-5908™	NCI-H1975	Non-small-cell lung carcinoma (NSCLC)	primary	CDKN2A, EGFR - L858R/T790M (c.2369C > T)



**Table 2:**

The effect of PCAIs on the viability of normal and lung cancer cells. The EC<sub>50</sub> values were obtained from concentration-response curves from 48 h of exposure to varying concentrations of PCAIs.

Cell line	EC <sub>50</sub> at 48 h (µM)						
	NSL-BA-036	NSL-BA-040	NSL-BA-055	NSL-BA-56	Docetaxel	Paclitaxel	Erlotinib
<b>A549</b>	8.9	5.2	5.6	49	>200	>200	>200
<b>NCI-H1573</b>	8.1	1.8	1.1	14	>200	>200	>200
<b>NCI-H661</b>	24	3.9	2.2	26	>200	11	>200
<b>NCI-H1975</b>	10	3.6	5.4	8.3	ND	ND	ND
<b>NCI-H1299</b>	5.4	5.5	5.2	12	72	60	>200
<b>NCI-H460</b>	11	4.6	6.2	26	56	26	>200
<b>NCI-H1563</b>	6.8	4.8	3.9	10	80	>200	>200
<b>WI-38</b>	6.8	6.6	6.2	9.0	ND	ND	ND